Paleoceanographic reconstructions from planktonic foraminifera off the Iberian Margin: Temperature, salinity, and Heinrich events

Olivia Cayre, Yves Lancelot,[1] and Edith Vincent[1]

Laboratoire de Géologie du Quaternaire du CNRS, Centre Européen de Recherche et d'Enseignement en Géosciences de l'Environnement, Aix en Provence, France

Michael A. Hall

Godwin Laboratory, University of Cambridge, Cambridge, England, United Kingdom

Abstract. A quantitative analysis of planktonic foraminifera in a core from the Iberian Margin allows a reconstruction of the evolution of oceanographic parameters during the last glacial cycle with a resolution of ~1000 years. A principal component analysis performed on 19 species allows the identification of 11 intervals characterized by increased abundances of the subpolar species. The youngest six of these intervals are correlated with the last 6 Heinrich events (HEs). The five cold events older than stage 4 are dated at 81, 90, 110, 129, and 140 ka, respectively. Paleotemperatures reconstructed using the modern analog technique indicate 4°C decreases during all even-numbered isotopic stages and stage 3. During the HEs, temperature decreases reach ~10°C and seawater $\delta^{18}O$ anomalies reach ~1‰. Temperature and salinity reconstructions indicate that the environment of the Iberian Margin has been under the combined influence of global factors such as the migration of the polar front and iceberg discharge and of regional factors such as the precipitation/evaporation regime on both oceanic and continental area.

1. Introduction

High concentrations of detrital elements in Quaternary sediment layers from the North Atlantic [*Pastouret et al.*, 1975; *Fillon*, 1985; *Heinrich*, 1988] have been interpreted as resulting from short periods of intense iceberg discharge and labeled Heinrich layers [*Broecker et al.*, 1992]. Transported by the anticlockwise polar gyre from the Laurentide [*Pastouret et al.*, 1975; *Heinrich*, 1988; *Bond et al.*, 1992] and Scandinavian [*Grousset et al.*, 1993; *Revel et al.*, 1996; *Elliot et al.*, 1998] ice sheets, icebergs encountering warm waters in the northeast Atlantic melt and release ice-rafted detritus (IRD). The last six Heinrich events (HEs) have occurred during the past 70 kyr and are now well documented in the North Atlantic [*Grousset et al.*, 1993; *Broecker*, 1994; *Bond and Lotti*, 1995; *Maslin et al.* 1995; *Cortijo*, 1995; *Manighetti et al.*, 1995; *Robinson et al.*, 1995; *Revel et al.*, 1996; *Rasmunssen et al.*, 1996, 1997; *Cortijo et al.*, 1997; *Elliot et al.*, 1998]. The southern limit of their extension remains uncertain. Although the southern portion of the Iberian Margin is located south of the position of the polar front during the Last Glacial Maximum (LGM), according to *Ruddiman and McIntyre* [1981], *Mix and Ruddiman* [1985], and *Ruddiman* [1987] (Figure 1) the influence of subpolar

conditions during short periods correlated with iceberg discharges has been shown [*Fatela*, 1995; *Lebreiro et al.*, 1996; 1997]. Moreover, the occurrence of IRDs in sediments has been reported as far south as the Portuguese and Moroccan Margins [*Kudrass and Thiede*, 1970; *Zahn et al.*, 1997]. HEs induce strong hydrographic changes in surface waters of the North Atlantic which have been reconstructed until a latitude of ~45°N [*Broecker et al.*, 1992; *Bond et al.*, 1992; *Sancetta*, 1992; *Thomas et al.*, 1995; *Maslin et al.*, 1995; *van Kreveld et al.*, 1996; *Auffret et al.*, 1996; *Cortijo et al.*, 1997; *Elliot et al.*, 1998]. The purpose of this paper is to estimate if all HEs have reached the southern Iberian Margin and to assess temperature, salinity, and productivity changes produced by these events at this latitude. Such changes can be reconstructed using the distribution of planktonic foraminifera in the sediment accumulations.

The surface circulation of the North Atlantic (Figure 1) mainly consists of an anticyclonic gyre which is represented in its northern part by the Gulf Stream and the North Atlantic Drift (NAD). The northern branch of the NAD brings warm and salty waters into the Norwegian, Greenland, and Arctic Seas whereas, in contrast, southerly currents bring cold and low-salinity waters into lower latitudes. The boundary between low-salinity polar waters and Arctic waters constitutes the polar front, and the boundary between cold Arctic waters and warm Atlantic waters constitutes the Arctic front. Linked with the different water masses, the foraminiferal fauna is divided in six assemblages called polar, subpolar, transitional, subtropical, tropical, and upwelling assemblages [*Bé and Tolderlund*, 1971; *Kipp*, 1976; *Pujol*, 1980; *Hemleben et al.*, 1988; *Ottens*, 1992; *Johannessen et al.*, 1994] (Figure 1). At midlatitudes the sea surface temperature (SST) is relatively
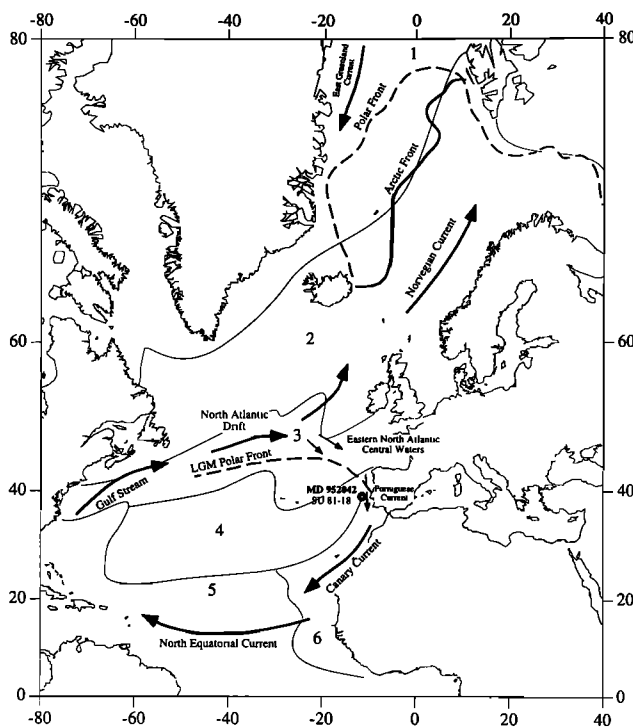
Figure 1. Surface circulation in the North Atlantic simplified from *Pickard and Emery* [1982]. Positions of modern polar and Arctic fronts are from *Johannessen et al.* [1994], and the position of the polar front for the Last Glacial Maximum (LGM) is from *Ruddiman and McIntyre* [1981]. Numbers 1-6 refer to planktonic foraminiferal provinces identified from plankton tows and surface sediments (data from *Bé and Tolderlund* [1971], *Pujol* [1980], *Hemleben et al.* [1988], *Ottens* [1992], and *Johannessen et al.* [1994]): 1, polar; 2, subpolar; 3, transitional; 4, subtropical; 5, tropical; and 6, upwelling assemblage.

easily and reliably derived from analyses of the planktonic foraminiferal fauna using transfer functions. Two methods are commonly used: that of *Imbrie* and *Kipp* [1971] and the modern analog technique (MAT) [*Hutson*, 1979; *Prell*, 1985; *Pflaumann et al.*, 1996]. Sea surface salinity (SSS) also can be estimated from transfer function in areas where it is independent from the SST [*Kipp*, 1976]. It is also commonly calculated from the oxygen isotopic composition of the foraminifera [*Duplessy et al.*, 1991, 1992, 1993; *Rostek et al.*, 1993; *Maslin et al.*, 1995]. Sea surface productivity can also be reconstructed by transfer function [*Kiefer et al.*, 1995; *Cayre et al.*, 1999] or using the foraminiferal accumulation rate [*van Kreveld et al.*, 1996].

During the cruise Images I of the R/V *Marion Dufresne* in July 1995 a 32.5 m piston core (MD 952042) was retrieved from the Iberian Margin off Portugal (37°48'N, 10°10'W) in 3146 m of water depth. The core offers a good potential for high-resolution analysis of the paleoceanographic evolution of the midlatitude North Atlantic. In our study a principal component analysis allows the identification of the succession of assemblages throughout the core. A reliable chronostratigraphy has been obtained by calibration of the oxygen isotopic composition of *Globigerina bulloides* with the stacked record of *Martinson et al.* [1987] and the nearby core SU 81-18 [*Bard et al.* 1987]. SSTs have been

reconstructed from transfer functions using MAT [*Hutson*, 1979; *Prell*, 1985], and paleosalinities are estimated from the $\delta^{18}O$ record. The foraminiferal accumulation rate is calculated to estimate the surface productivity during HE1.

2. Material and Method

Core MD 952042 consists mainly of an alternation of clayey mud and carbonate ooze. Only the upper 30 m of the core were sampled because sediments in the lower 2.5 m show evidence of coring disturbance. Samples were taken every 10 cm between 3 and 6 m and every 20 cm throughout the remainder of the core. Samples 1 cm thick and corresponding to ~10 g of sediments were dried, weighed, and washed over a 63 μm mesh sieve. The >63 μm residue was dried and weighed. The core was recovered well above the carbonate compensation depth, and no trace of dissolution was observed on whole foraminiferal tests.

Twenty specimens of *G. bulloides* from the 250-350 μm fraction were handpicked from all samples for measurement of their oxygen and carbon isotopic composition. The foraminiferal tests were immersed into hydrogen peroxide for 30 min, crushed, and ultrasonically cleaned for 20 s in acetone. The floating part was removed, and foraminifera were dried at 50°C. Isotopic measurements were performed at the Godwin Laboratory (University of Cambridge, Cambridge, United Kingdom) on a VG Isogas SIRA mass spectrometer with automatic carbonate preparation system. Calibration to the Vienna Peedee Belemnite (PDB) standard is via the National Bureau Standards (NBS)-19 standard. Analytical precision is better than 0.1‰.

Counts of the planktonic foraminiferal fauna were conducted on samples collected every 20 cm. The >150 μm fraction was split until an appropriate quantity of foraminifera was obtained for counting. One of the two last splits was distributed on a gridded tray. About 350 planktonic foraminifera were picked in a known number of squares, identified, glued on a micropaleontological slide, and counted according to the Climate: Long-Range Investgation, Mapping, and Prediction (CLIMAP) taxonomy [*Kipp*, 1976].

Foraminiferal assemblages were identified by principal component analysis (PCA) using the relative abundance of 19 species in 150 samples. The PCA is a descriptive statistical method which determines the resemblance between individuals (sediment samples in this study) and linear links between variables (planktonic foraminiferal species). The PCA fits the set of points in order to obtain the best representation in a subspace (usually in two dimensions). The first factorial axis has the maximum inertia; the next axes are perpendicular with decreasing inertia. We use a standardized PCA where variables are of mean 0 and variance 1, so that the most or the least abundant species have the same influence to calculate distances between individuals. Calculations were obtained via MacMul and GraphMu software [*Thioulouse*, 1990].

Paleo SSTs were reconstructed from planktonic foraminifera using the transfer function MAT [*Hutson*, 1979; *Prell*, 1985]. The database contains 617 core tops covering the North Atlantic [*Pflaumann et al.*, 1996]. The MAT is based on the dissimilarity coefficient (squared chord distance) existing between each fossil sample of the core and core tops

of the database. The mean SSTs of August and February associated with each fossil sample were calculated from the 10 best modern analogs (minimum dissimilarity coefficient).

Paleo SSSs were estimated from the $\delta^{18}O$ record. The oxygen isotope ratio in planktonic foraminifera shells reflects the temperature and salinity of the water where calcification occurs and is also dependent on global ice volume. Subtracting the effect of temperature and global ice volume, it is possible to calculate the $\delta^{18}O$ anomaly due to the salinity [Duplessy et al., 1991,1992; Rostek et al., 1993]. Erez and Luz [1983, equation (1)] enables us to calculate the seawater $\delta^{18}O$ from the global $\delta^{18}O$ and the temperature of calcification.

$$T = 17 - 4.52(\delta^{18}O_{carbonate}-\delta^{18}O_{seawater})$$

$$+ 0.03(\delta^{18}O_{carbonate} - \delta^{18}O_{seawater})^2 \qquad (1)$$

The SST obtained by transfer function does not necessarily correspond to the temperature of calcification of the species on which the $\delta^{18}O$ is measured (because of the seasonal and/or depth habitat signal recorded by the $\delta^{18}O$). Duplessy et al. [1992] showed that in the North Atlantic the oxygen isotopic record of G. bulloides corresponds to a calcification temperature between 7° and 22°C and that the estimated SST must be corrected by -1°C ($T°C$ calcification = $T°C$ $_{August}$-1). Since our estimates lie in the specified temperature range (except for very short periods) we used the August temperature minus 1°C in (1). The temperature anomaly was then calculated by subtracting the modern $\delta^{18}O$ value from the past ones. The impact of the global ice volume was calculated by Labeyrie et al. [1987]. We normalized their results to the value of 1.2‰ for the LGM/Holocene transition, established with the calibration of the ^{14}C-dated Barbados sea level curve of Fairbanks [1989]. Our $\delta^{18}O$ record and the global ice volume record are linearly interpolated with an interval of 200 years in order to have the same resolution. The seawater $\delta^{18}O$ anomaly obtained after subtracting the temperature and global ice volume anomalies results from salinity changes. These salinity changes can be induced by local changes in the precipitation-evaporation balance affecting the freshwater runoff from the continent and/or by inputs of freshwater from ice sheet melting. Since equations used to estimate the salinity from the seawater $\delta^{18}O$ anomaly include many approximations and have different slopes when due to changes in the precipitation-evaporation balance rather than inputs of freshwater, we will discuss only our results in terms of the seawater $\delta^{18}O$ anomaly.

The occurrence of IRD in the sediments was analyzed by a qualitative study of the >150 μm fraction. Minerals were summarily identified, and their abundance was estimated visually, according to four rankings: rare, present, abundant, and dominant.

3. Results

3.1. Isotopic Stratigraphy

The $\delta^{18}O$ record of core MD 952042 covers the last glacial cycle (Figure 2b). Isotopic stages are identified by comparison with the stacked isotope record of Martinson et
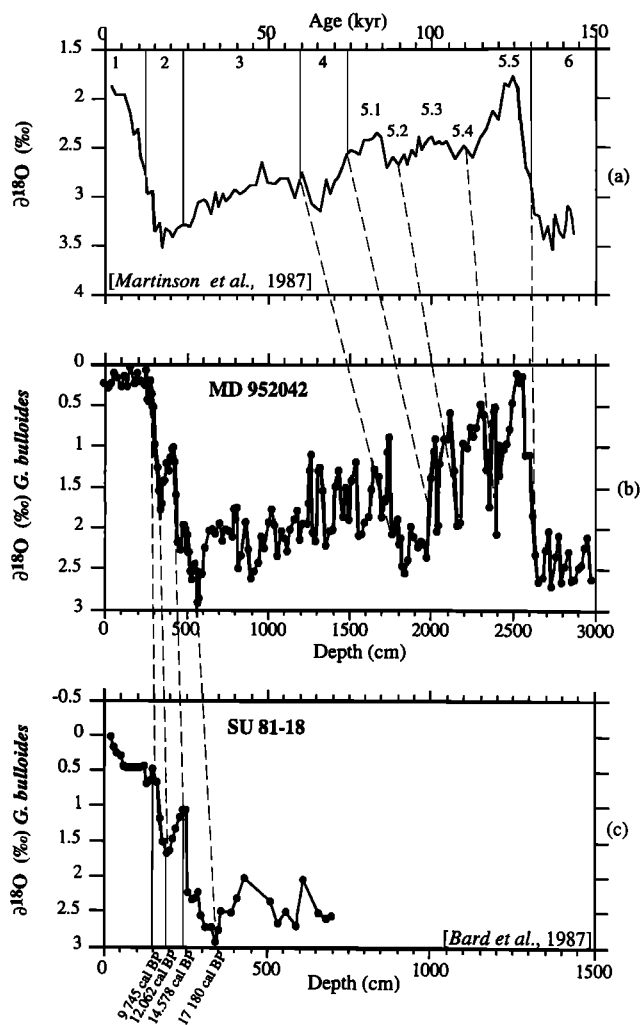

Figure 2. Oxygen isotopic stratigraphies. (a) The stacked record of Martinson et al. [1987] as a function of time. Numbers above the curve refer to isotopic stages. (b) The $\delta^{18}O$ values for Globigerina bulloides in core MD 952042 (37°48'N, 10°10'W) as a function of depth. (c) The $\delta^{18}O$ values for G. bulloides in core SU 81-18 (37°46'N, 10°11'W) as a function of depth [Bard et al., 1987].

al. [1987] (Figure 2a). All stages and boundaries are easily identifiable except the transition 3/2. The Younger Dryas (YD) is well marked by a $\delta^{18}O$ maximum at 340 cm. The decrease of the Bölling period (410 cm) does not reach the values of the Holocene period. The amplitudes of the $\delta^{18}O$ steps at the transition 2/1 and 6/5 reach 2.65‰ and 2.50‰, respectively. Glacial interstadials of stage 5 (corresponding to stages 5.2 and 5.4 following the Martinson's event nomenclature) are characterized by values ~2‰ higher than interglacial interstadials (stages 5.5 and 5.3). Oscillations of 1.5‰ occur during stage 3.

The $\delta^{18}O$ record of core MD 952042 is compared to that of the nearby core SU 81-18 (37°46'N, 10°11'W) [Bard et al., 1987, 1996] for the last deglaciation (Figure 2c). Both cores reach $\delta^{18}O$ values near 3‰ for the LGM, which decrease down to 1‰ in the Bölling period. An increase of ~0.7‰ characterizes the YD in both cores, and Holocene values are

Table 1. Chronostratigraphy of Core MD 952042

Depth in Core MD 952042, m	Depth in Core SU 81-18, m	Isotopic Event[a]	Ages, kyrs
2.80	1.40		9.7[b]
3.40	1.80		12.1[b]
4.20	2.30		14.6[b]
5.70	3.30		17.2[b]
17.60		4/3	59.0[a]
19.80		5/4	73.9[a]
21.60		5b	91.0[a]
24.00		5d	110.8[a]
26.20		6/5	129.8[a]

[a] From *Martinson et al.* [1987]

[b] Calendar ages from core MD 81-18 [*Bard et al.*, 1987, 1996], which correspond to ^{14}C datings at 8.76, 10.28, 12.26, and 14.59 ka, respectively.

near 0.5‰. Both cores record an increase from 2 to 3‰ just before the LGM.

3.2. Age Model

For the interval spanning stages 6-4 the age model for core MD 952042 (Table 1) is based on ages of isotopic boundaries given by *Martinson et al.* [1987]. For the Holocene and the last deglaciation we used the ages of core SU 81-18 (located ~3 miles from core MD 952042) derived from more than 22 accelerator mass spectrometry (AMS)-^{14}C ages converted in calendar ages [*Bard et al.*, 1987, 1996].

The $\delta^{18}O$ record of stage 3 of core MD 952042 shows a rapid alternation of glacial and interglacial values. It could be tempting to try to relate those to the "Dansgaard-Oeschger" events (DO) [*Broecker and Denton*, 1989] detected in the Greenland Ice Core Project (GRIP) ice core [*Dansgaard et al.*, 1982, 1993; *Bond et al*, 1992; *Johnsen et al.*, 1992], but synchroneity cannot be established because the resolution as well as the chronological databases are very different in the two records.

3.3. Sedimentation Rate

Sedimentation rates have been calculated assuming a constant accumulation between the dated levels (Figure 3). For the entire core the sedimentation rate has an average value of 21 cm kyr^{-1}, but there are large variations between the different stages. The minimum rate occurs during stage 5 with values as low as 12 cm kyr^{-1}; it increases to 15 cm kyr^{-1} for stage 4 and to 28 cm kyr^{-1} in stages 3 and 2 below the LGM. The sedimentation rate reaches the value of 58 cm kyr^{-1} during the last deglaciation and decreases to ~30 cm kyr^{-1} for the Holocene. A marked increase in sedimentation rate during the deglaciation is in agreement with previous studies on cores from the same area [*Bard et al.*, 1987; *Cremer et al.*, 1992], but values obtained for the Holocene and the deglaciation in our core are surprisingly high. The comparison of the sedimentation rates of core MD 952042 with those of core SU 81-18 [*Bard et al.*, 1987] indicates that the sedimentation rates in core MD 952042 are ~30-40% higher than in core SU 81-18 (Figure 3). It appears that the sedimentation rate in core

MD 952042 is overestimated for the first meters of the core because of coring artefacts. A study of magnetic properties shows that the core is stretched in the upper 14-15 m with a maximum effect on the first 10 m (N. Thouveny and E. Moreno, personal communication, 1996). No disturbance of sediment structure was visually observed during the description of the core, and both the isotopic and magnetic records show no evidence of stratigraphic disturbance. It appears that stretching of the upper part of the core occured during the penetration of the core barrel into the upper soft layers under the influence of an excessive aspiration caused by rapid upward motion of the piston accompanying a rebound in the kevlar cable. The excess material that was incorporated in the core must have entered the barrel in the normal stratigraphic successsion without changing noticeably the stratigraphy or the compostion of the sediment. We constructed a sedimentation rate model assuming that cores MD 952042 and SU 81-18 should have approximately the same sedimentation rates. Between the Holocene and the LGM we took the sedimentation rate values from core SU 81-18; between the LGM and the transition 4/3 we took a mean value of 22 cm kyr^{-1}; and for sediment older than transition 4/3 we took values obtained in core MD 952042.

3.4. Coarse Fraction: Absolute Foraminiferal Abundance and Lithogenic Inputs

The percentage of the coarse fraction (>63 μm) shows a correlation with the $\delta^{18}O$ record with high percentages of ~4-6% occurring during interglacial stages and low values of 1% during glacial stages (Figure 4a). Foraminiferal abundance in the bulk sediment correlates rather well with the coarse fraction, indicating that planktonic foraminifera are, in most samples, the main component of the coarse fraction (Figures 4a and 4b). High values of coarse fraction corresponding with low values of foraminiferal abundance indicate coarse detrital inputs. The relatively low values (near 900 forams g^{-1}) shown at the end of the Holocene result from dilution by abundant iron sulfide concretions. Peaks of coarse fraction at 9.60 and between 27 and 28 m result from the presence of indurated clay aggregates and ferric concretions or from the occurrence of organic tubes mineralized by iron sulfides. Rounded quartz grains suggesting ice transport are abundant between 4.80 and 5.20 and at 8.40, 13.80, and 15.80 m. They are present at 18.10 m and rare at 11.00 m. Volcanic ash is present in
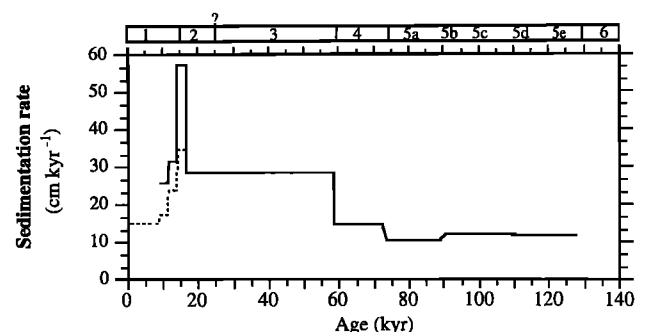

Figure 3. Sedimentation rates in cores MD 952042 (solid line) and SU 81-18 (dashed line). Isotopic stages are indicated at the top.
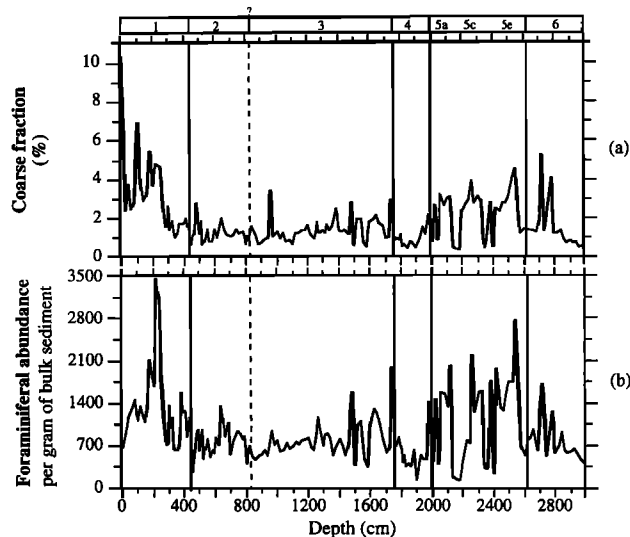
Figure 4. Percentage of the (a) >63 μm sediment fraction and (b) foraminiferal abundance in the bulk sediment as a function of depth in core MD 952042. Isotopic stages are indicated at the top.

samples near 11.00 and 18.10 m and abundant in samples at 20.00, 21.60, 26.20, and 29.80 m.

3.5. Planktonic Foraminiferal Assemblages

The first and second axes of the PCA, computed from foraminiferal counts in core samples, account for 23 and 17% of the total inertia, respectively, and they define three assemblages (Figure 5). The first assemblage contains *Globigerinoides ruber, Globigerinoides sacculifer, Globigerinoides tenellus, Globigerinoides conglobatus, Globoturborotalita rubescens*, left- and right-coiling *Globorotalia truncatulinoides, Globorotalia crassaformis*, and

Globigerinella aequilateralis. The second assemblage contains *Orbulina universa, Globigerina falconensis, Globigerinita glutinata, Globigerinella calida, Globorotalia inflata, Globorotalia hirsuta, Neogloboquadrina dutertrei*, and right-coiling *Neogloboquadrina pachyderma*. The third assemblage consists of left-coiling *N. pachyderma, Turborotalita quinqueloba* and *G. bulloides*. According to their species composition the first and third assemblages belong to the subtropical and subpolar provinces, respectively (Figure 1). The second assemblage contains species characteristic of transitional or upwelling areas.

The abundance of the subtropical assemblage is maximum during the Holocene and during warm periods of stage 5, whereas the transitional/upwelling assemblage is maximum during glacial stages and interstadials except during short intervals where the subpolar assemblage increases drastically (Figure 6). Although in the PCA results *G. bulloides* belongs to the same group as the two subpolar species left-coiling *N. pachyderma* and *T. quinqueloba*, its distributional trends in the core are different from those of the two latter species (Figure 7). Throughout the core, *G. bulloides* represents an average of ~15% of the total foraminiferal population and never drops below 12%, whereas the two other subpolar species are nearly absent during warm periods and show significant and abrupt increasing abundances during short intervals. Increases of *G. bulloides* are not necessarily synchronous with those of the subpolar species, and the amplitudes of increases are often different. In the North Atlantic, *G. bulloides* seems to proliferate in nutrient-poor environments, where other species cannot grow for various reasons [*Pujol*, 1980]. In core MD 952042, peaks of abundance of *G. bulloides* usually occur during a transitional period just after or before a stable (warm or cold) period. The two subpolar species left-coiling *N. pachyderma* and *T. quinqueloba* are dominant at the end of stage 6, during substage 5b, stage 4, and short events of stages 3 and 2, and just before the deglaciation. Their last increase occurs during the YD.
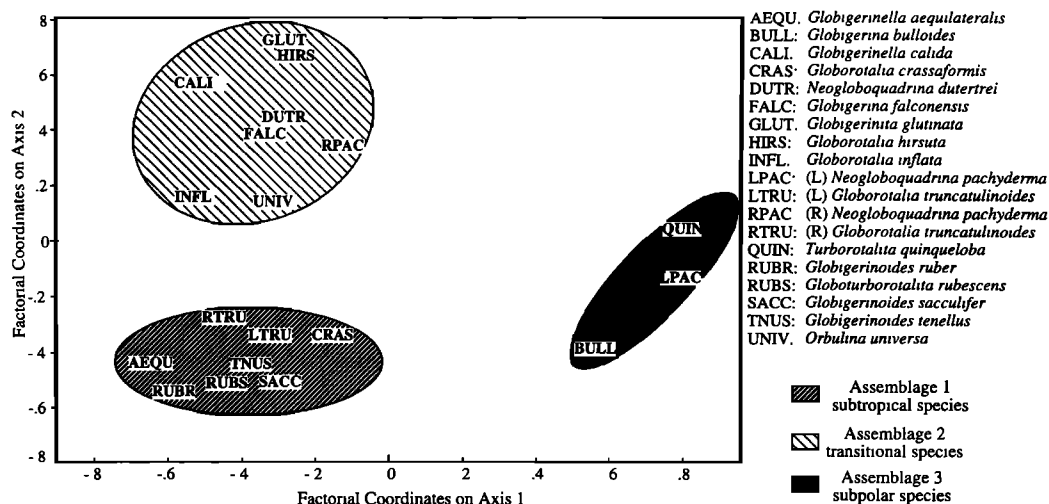

AEQU. *Globigerinella aequilateralis*
BULL: *Globigerina bulloides*
CALI. *Globigerinella calida*
CRAS· *Globorotalia crassaformis*
DUTR: *Neogloboquadrina dutertrei*
FALC: *Globigerina falconensis*
GLUT. *Globigerinita glutinata*
HIRS: *Globorotalia hirsuta*
INFL. *Globorotalia inflata*
LPAC· (L) *Neogloboquadrina pachyderma*
LTRU: (L) *Globorotalia truncatulinoides*
RPAC (R) *Neogloboquadrina pachyderma*
RTRU: (R) *Globorotalia truncatulinoides*
QUIN: *Turborotalita quinqueloba*
RUBR: *Globigerinoides ruber*
RUBS: *Globoturborotalita rubescens*
SACC: *Globigerinoides sacculifer*
TNUS: *Globigerinoides tenellus*
UNIV. *Orbulina universa*

Assemblage 1 subtropical species
Assemblage 2 transitional species
Assemblage 3 subpolar species

Figure 5 Foraminiferal assemblages defined by the principal component analysis (PCA) in the 150 samples of core MD 952042 with 19 planktonic foraminiferal species. Factorial coordinates on axes 1 and 2 correspond to the factor score of each species in relation to factor 1 and factor 2, respectively.
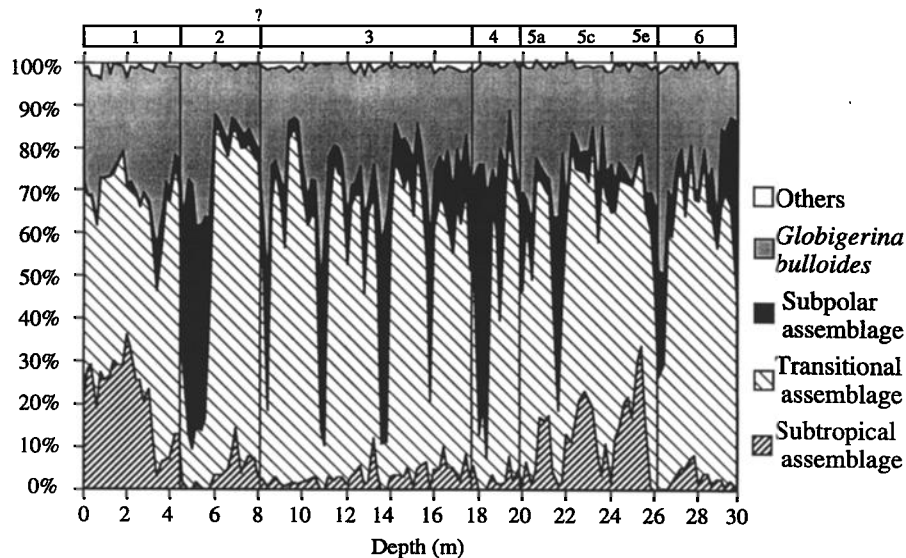
Figure 6. Percentages of the foraminiferal assemblages in core MD 952042 as a function of depth. Isotopic stages are indicated at the top.

3.6. Characterization of the Heinrich Events

Eleven short intervals of abrupt cooling are identified by the dominance of the subpolar foraminiferal assemblage. They correspond to the following depths down the core: between 4.80 and 5.20 m and near 8.40, 11.00, 13.60, 15.80, 18.10, 20.00, 21.60, 23.60, 26.20, and 29.80 m. They are labeled c1-c11 in Figure 7. The coarse fractions of these intervals contain IRDs and exhibit high and sharp peaks in magnetic susceptibility [*Candon et al.*, 1996] (Figure 7d). The magnetic susceptibility peaks identified in core MD 952042 are believed to result from the presence of iron-rich detrital grains coming from the Canadian belt. Thus the six youngest periods of intense cooling can be identified as the six HEs described in the literature [*Heinrich*, 1988; *Broecker et al.*, 1992; *Bond et al.*, 1992; *Grousset et al.*, 1993; *Cortijo*, 1995; *Maslin et al.*, 1995; *Robinson et al.*, 1995; *Revel et al.*, 1996; *van Kreveld*, 1996; *van Kreveld et al.*, 1996; *Rasmunssen et al.*, 1997]. The five oldest major coolings recorded by planktonic foraminifera (called c7-c11 in Figure 7) occur at the end of stage 5, during interstadials 5b and 5d, just before the transition 6/5, and at the bottom of the core, respectively. Our record is similar to those described by *Heinrich* [1988] and by *Grousset et al.* [1993]. Events c7, c8 and c10, however, have not been reported in sediment cores from the NE Atlantic [*Manighetti et al.*, 1995; *van Kreveld et al.*, 1996].

Following our chronology, the last six HEs are dated 16, 27, 35, 45, 52, and 64 ka (Table 2), respectively. The calendar age of HE1 in our study corresponds to about the calendar age obtained after transformation of the ^{14}C age of this event in most recent studies. HE2 and HE3 are older than in other studies, but our chronology has no dated point between the beginning of stage 3 and the LGM. The calendar age of HE4 is in agreement with that from *Manighetti et al.* [1995], whereas the calendar ages of HE5 and HE6 are near those attributed to *Bond et al.* [1992, 1993]. Events c7, c8, c9, c10, and c11 are dated 81, 90, 110, 129, and 140 ka (Table 2), respectively. Events c7, c8, c9, and c10 correspond to events h7, h8, h10,

and h11 of *Heinrich* [1988], and c10 also corresponds to event H7 of *Manighetti et al.* [1995] (Table 2). These events have also been detected over the North Atlantic by peaks in magnetic susceptibility [*Robinson et al.*, 1995]. In the South Atlantic, *Little et al.* [1997] noted two events, at 95 and 110 ka, that have characteristics similar to those leading the North Atlantic HEs.

4. Paleoceanographic Reconstructions

4.1. Paleotemperatures

Average SSTs reconstructed for the Holocene oscillate around 16.6° ± 1.5°C in winter and 21.3° ± 1.2°C in summer (Figure 8) and are slightly warmer than temperatures measured today [*Levitus*, 1982], which are 15.1° and 20.3°C, respectively. The discrepancy between estimated and measured SSTs is not significant. It results from using some modern analogs coming from the Mauritanian Coast where SST is near 18.0°C in winter and 22.0°C in summer (in addition to core tops coming from the Iberian Coast). The YD is characterized by a cooling down to 11.7° ± 2.0°C in winter and 17.7° ± 2.0°C in summer. During the Bölling period, SSTs reach, and even exceed, Holocene values. These reconstructed high SSTs result again from modern analogs coming from the West African Coast. The occurrence of the subpolar assemblage just before the deglaciation indicates SSTs near 5.0° ± 1.0°C in winter and 10.0° ± 1.5°C in summer. The best analogs for that period are found at ~58°N and 45°W (SE Greenland). All intervals dominated by the subpolar assemblage yield similar low reconstructed SSTs. Mean SSTs during stages 2, 3, and 4, calculated after removal of these cold intervals, remain between 12° and 13°C in winter and 17° and 18°C in summer and are in agreement with the glacial temperatures estimated by CLIMAP [*CLIMAP Members*, 1981; *Prell*, 1985]. The best analogs for these stages are found between 42° and 50°N in the central east Atlantic. Reconstructed temperatures during warm periods of stage 5 compare well to those obtained for the
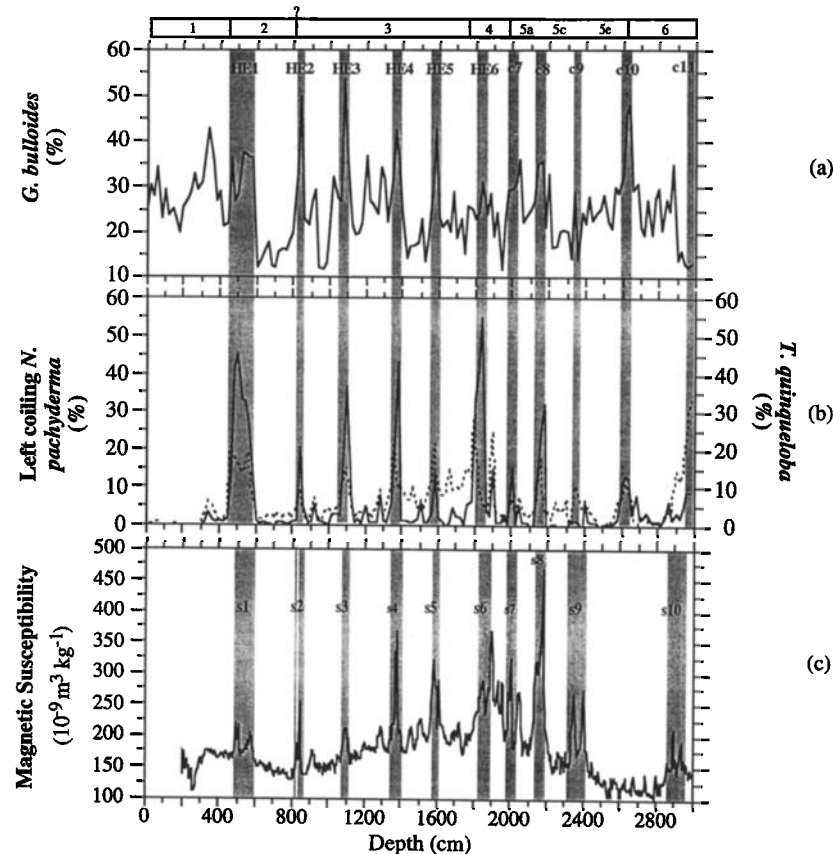
Figure 7. Percentages of planktonic foraminiferal species in core MD 952042: (a) *G. bulloides*, (b) left-coiling *Neogloboquadrina pachyderma* (solid line) and *Turborotalita quinqueloba* (dashed line) (shaded intervals correspond to the last six HEs and the five older coolings, c7-c11), and (c) magnetic susceptibility [*Candon et al.*, 1996] (shaded intervals with high susceptibility values are labeled s1-s10). Isotopic stages are indicated at the top.

Holocene. Except for the rapid cooling occurring just before transition 6/5, SSTs for stage 6 are ~12°C in winter and 17°C in summer; they are quite similar to those of stage 2.

All the coolings recorded correspond to a temperature decrease of ~8°C, except those occurring during the YD and during stage 5d where the temperature drop reaches only 4°C.

For stage 5d the signal recorded by the magnetic susceptibility is similar to those recorded during other cold events. The event being very short and corresponding to a period of very low foraminiferal abundance, the bioturbation can dilute the cold foraminiferal signal. For the YD, despite the fact that cores MD 952042 and SU 81-18 have similar

Table 2. Ages Attributed to Heinrich Events (HE) and to Cold Events Older Than HE6 in This Study Compared to Those Obtained by *Heinrich* [1988], *Bond et al.* [1993], *Cortijo* [1995], *Manighetti et al.* [1995], *Kiefer* [1997], *Little et al.* [1997], *Voelker et al.* [1998], and *Elliot et al.* [1998]

Event	This Study Calendar Ages	Heinrich [1988] Calendar Ages	Bond et al. [1993] 14C Ages	Cortijo [1995] 14C Ages	Manighetti et al. [1995] 14C Ages	Manighetti et al. [1995] Calendar Ages	Kiefer [1997] 14C Ages	Little et al. [1997] Calendar Ages	Voelker et al. [1998] 14C Ages	Elliot et al. [1998] 14C Ages
HE1	16	11	14	14	15	17	14		14	15
HE2	27	22	21	21	22	25	21		21	22
HE3	35	32	27	28	28	31	26		26	27
HE4	45	48	35	35	39	43	34		34	35
HE5	53	59	50[a]	44		55			44	
HE6	64	71	66[a]			70			>51	
C7	76	(h7) 80								
C8	91	(h8) 91						(PS7) 95		
C9	111	(h10) 112						(PS8) 110		
C10	129	(h11) 128								
C11	140									

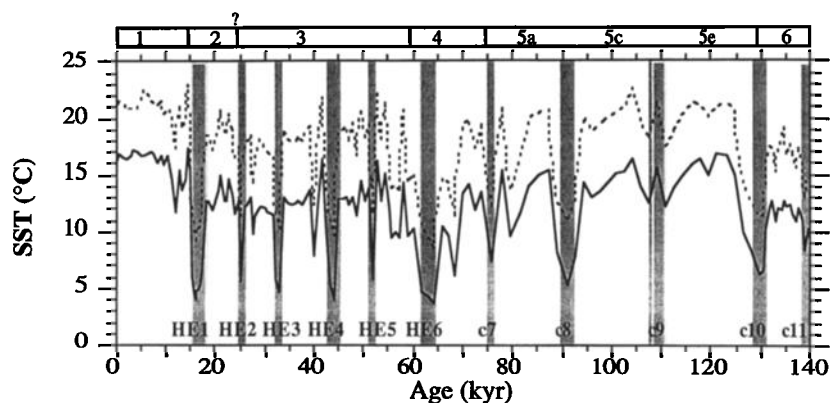[a] Calendar ages after *Bond et al.* [1992].

Figure 8. August (dashed line) and February (solid line) sea surface temperature (SST) reconstructed by the modern analog technique for core MD 952042. Isotopic stages are indicated at the top.

$\delta^{18}O$ records the cooling recorded in core SU 81-18 [*Bard et al.*, 1987] is more pronounced than in our core since the temperature for the YD reaches 7°C in winter and 14°C in summer. Similar temperature reconstructions are obtained in core SU 9228 (37°05'N, 09°28'W) [*Boelaert*, 1998]. The discrepancy between the records in the different cores does not result from the methods used for the temperature reconstructions but from a real difference in the percentage of foraminiferal species. In core MD 952042 a mixing with reworked sediment from stages 2 or 3, where the temperature is ~14°C in winter and 18°C in summer, could induce an apparent increase of the temperature of YD interval associated with a small increase of the $\delta^{18}O$. The presence of reworked sediment in the interval corresponding to the YD has been detected by AMS-^{14}C dating in core SU 81-14 (36°46'N, 9°51'W) [*Bard et al.*, 1989], and similar analyses should be performed on our core in order to confirm our hypothesis.

4.2. Paleosalinities

We subtracted the $\delta^{18}O$ anomalies due to the temperature (Figure 9b) and the $\delta^{18}O$ anomaly due to change in ice volume (Figure 9c) from the oxygen isotope values of *G. bulloides* (Figure 9a). The resulting seawater $\delta^{18}O$ anomaly (Figure 9d) shows a very good correlation with the temperature record. The major coolings recorded by planktonic foraminifera at various levels such as the bottom of the core, the transition 6/5, substage 5b, the end of stage 5, and the six HEs correspond to periods of strong decrease in salinity. During most of stage 5, with the exception of abrupt short duration coolings, the salinity is about equal to that of the modern day. The beginning of stage 4 is characterized by a major positive seawater δ^{18} anomaly (+1.2‰) followed by a rapid salinity decrease preceding the major one associated with HE6. Again, except for the short duration coolings, stages 3 and 2 seem on the average just slightly saltier than the Holocene, and the seawater $\delta^{18}O$ anomaly has a mean value of +0.5‰. During the six HEs and the older cooling events the salinity anomalies reach values between -0.8 and -2.1‰. The strongest negative anomaly corresponds to HE1 and is similar to the anomaly reconstructed by *Duplessy et al.* [1993] for the same period in core SU 81-18. The $\delta^{18}O$ salinity anomalies

calculated for HEs are also in agreement with those calculated by *Cortijo et al.* [1997] for HE4 in two cores at 38° and 40°N. It can be noted that the small temperature decrease of the YD in our record leads to a salinity increase in contrast with the salinity decrease evidenced in core SU 81-18 [*Duplessy et al.*, 1993]. The difference between the two records (which have similar $\delta^{18}O$ signals) can be explained by the gap of 3°C in the August temperature. Similarly, during substage 5d (event c9) the temperature decrease of 4°-5°C is not accompanied by a major salinity decrease.

5. Discussion: Evolution of the Environment off the Iberian Margin During the Last Glacial Cycle

The variations of oceanic parameters recorded in the sediments from core MD 952042 allow a tentative reconstruction of the evolution of the environment off the Iberian Margin during the past 140 kyr. The record suggests that during that period the Iberian Margin has been under the combined influence of three different factors, namely, (1) migration of the polar front, (2) iceberg discharge events, and (3) evolution of the climate on the adjacent continent.

The large-amplitude coolings observed in the surface waters off Portugal during the past 140 kyr are associated with strong salinity decreases generally corresponding with periods of large influx of low-salinity waters during major ice surges of continental ice sheets, as in most of the North Atlantic. The six youngest of these events are well documented by both signals, and also correspond with the presence of IRDs in the sediments. Therefore they are believed to represent a southern extension of the six HEs. Recently, three of the youngest HEs (HE1, HE2, and HE4) have been identified at approximately the same latitude as core MD 952042 in a shorter core taken on the Portuguese Margin in 1099 m of water depth [*Zahn et al.*, 1997] whereas HE1, HE2, HE3, HE4, and HE6 have been identified on the Tore Seamount (39°N, 12°W) [*Lebreiro et al.*, 1996]. Our observations fully document the occurrence of all of the six HEs as far south as 37°48'N. Furthermore, the five older cold events, which we have labeled c7-c11, are also characterized by strong coolings and salinity decreases. They
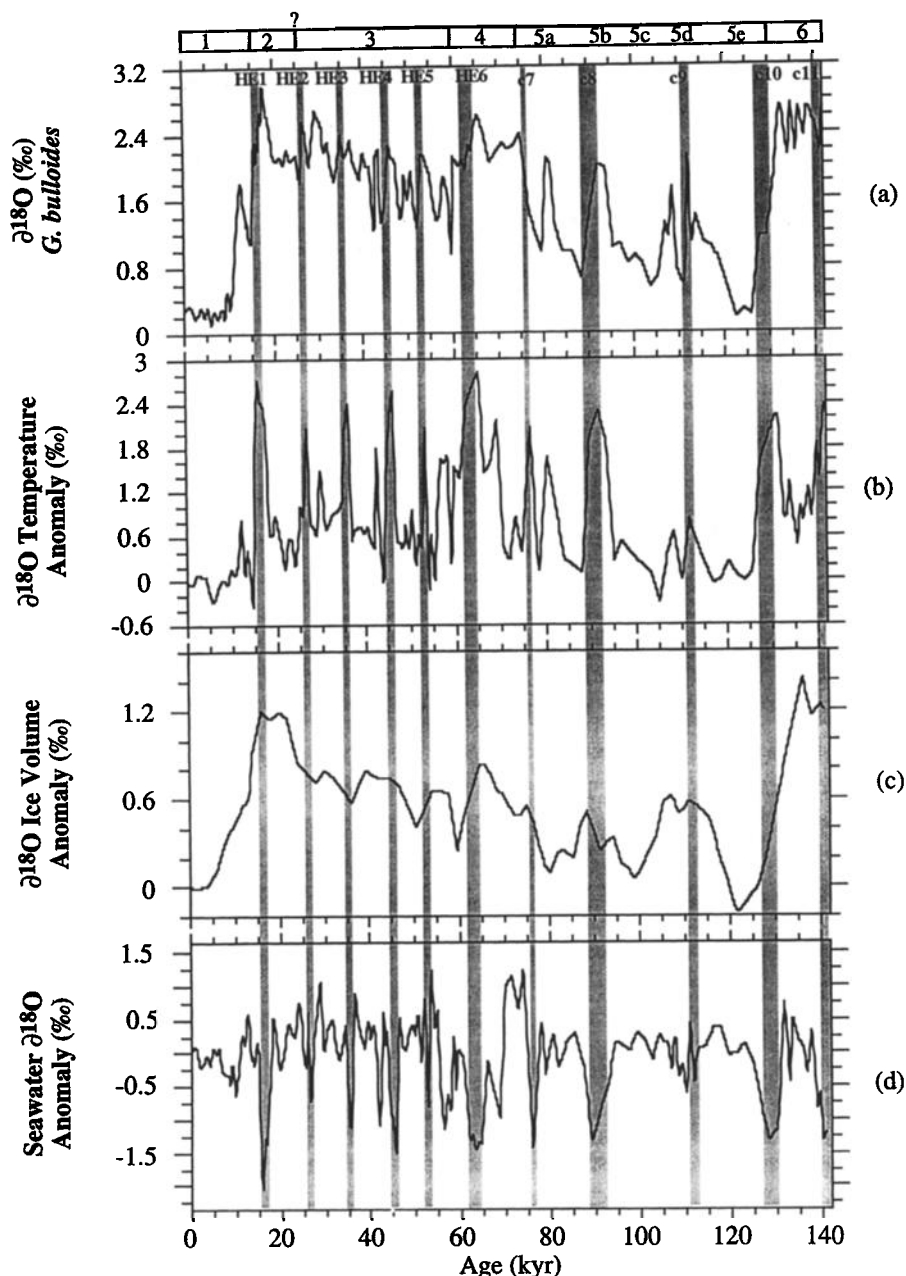
Figure 9. (a) The $\delta^{18}O$ values for *G. bulloides* in core MD 952042 as a function of age. (b) The $\delta^{18}O$ anomaly due to the temperature calculated from the equation of *Erez and Luz* [1983] using the August reconstructed temperature minus 1 [*Duplessy et al.*, 1992]. (c) The $\delta^{18}O$ anomaly due to the global ice volume [*Labeyrie et al.*, 1987] normalized to 1.2‰ for the LGM after *Fairbanks* [1989]. (d) The $\delta^{18}O$ anomaly due to the salinity obtained by subtracting the $\delta^{18}O$ temperature and ice volume anomalies from the $\delta^{18}O$ record of *G. bulloides*. Isotopic stages are indicated at the top, and shaded intervals are those dominated by the subpolar assemblage.

occur at the end of stage 6, just before transition 6/5, during interstadials 5d and 5b, and near the transition 5/4, respectively, and are interpreted as equivalent to older HEs. Other cold events occurring during stage 3 (between HE3 and HE4 and between HE5 and HE6) also exhibit a good correlation between salinity and temperature minima. Since they lack IRDs, however, they are not considered typical HEs, although they may result from hydrological conditions

similar to those prevailing during the HEs. They can be at midlatitude the expression of some of the millenial-scale iceberg discharges detected in high latitudes [*Bond et al.*, 1997; *Elliot et al.*, 1998].

In general, if we discard the abrupt coolings and the corresponding sharp salinity minima, the average salinity relative to the mean ocean salinity appears to have varied only slightly and remains comparable to that of the Holocene

for the entire period studied here, even during stage 6. Notable exceptions occur during stage 4 where salinity increases strongly and, to a lesser extent, during stages 3 and 2. Salinity increases can be attributed to an advection of tropical water, enhanced oceanic evaporation, and/or regional drought affecting both the continent and oceanic areas. As the major positive seawater $\delta^{18}O$ anomalies do not correspond to significant warmings, the hypothesis of an advection of tropical water (more saline and warmer water) must be rejected. An increased aridity is documented by the pollen record from southern Spain during stage 4 [*Pons and Reille*, 1988], and we thus favor a change in the evaporation/precipitation regime on the oceanic and continental areas to induce salinity increases at the beginning of stage 4. This high-salinity episode terminates abruptly with a strong decrease in both temperature and salinity preceding HE6. This decrease corresponds to a peak in magnetic susceptibility and could be equivalent to an HE. Salinity increases characterizing stages 3 and 2 have a lower amplitude than at the beginning of stage 4. Most continental records associate glacial stages with low rainfall periods, and as for stage 4, we attribute the salinity increases to variations in the regional precipitation/ evaporation regime.

During the HEs the climatic signal is dominated by the migration of the polar front and by iceberg discharge. Quantitative analysis of the foraminiferal fauna reveals some of the cold episodes (Figure 7). In HE1, HE4, and HE6, *T. quinqueloba* is seen to increase (20-28%) at the end of the events after the domination of left-coiling *N. pachyderma* (46-56%). High percentages of *T. quinqueloba* (>20%) are characteristic of the Arctic front in the modern North Atlantic [*Johannessen et al.*, 1994], and high abundances of left-coiling *N. pachyderma* characterize polar waters. These suggest that planktonic foraminiferal assemblages may have recorded the installation of a polar environment, followed by its northward migration at the end of the cold event. The cooling at the beginning of the HEs seems abrupt while warming seems more gradual, and the first warming step is characterized by an increase of *T. quinqueloba* which may correspond to the passage of the Arctic front.

During HE2, HE3 and HE5 the foraminiferal assemblage is dominated by *G. bulloides* (45-55%), suggesting a slightly less intense cooling. For HE5 the second most abundant species is *T. quinqueloba* (22%), indicating that the core location was probably near the Arctic front. Our study indicates that quantitative analysis of foraminiferal species can be efficiently used to reconstruct the past position of the Arctic and polar fronts. It also shows that HE1 and HE6 (and maybe HE4) produce the most intense coolings while HE2 occurs during the maximum volume of ice caps near 21 ka. Our results have to be confirmed by a very high resolution study in the Heinrich layers in order to characterize more precisely the different steps recorded for each HE.

Considering the foraminiferal accumulation rate as a productivity indicator, we estimated productivity changes only during HE1 since we do not have reliable sedimentation rates throughout other HEs. Foraminiferal accumulation rates exhibit productivity decreases at the beginning and at the end of HE1 whereas the productivity seems relatively high during the event (Figure 10). High foraminiferal productivity during
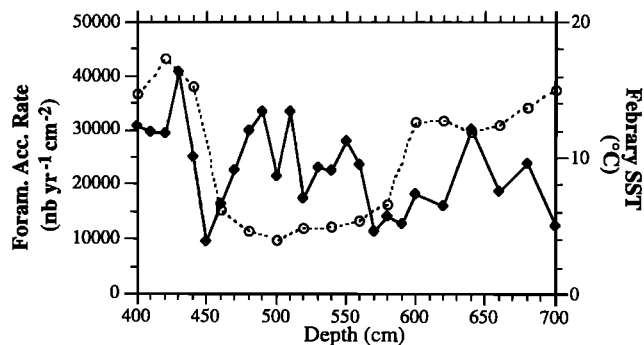

Figure 10. Foraminiferal accumulation rate (solid diamonds) and SST (open circles) throughout HE1.

HEs has been evidenced in the Irminger Basin [*Elliot et al.*, 1998] as well as in other parts of the IRD belt [*Kiefer et al.*, 1995; *Chapman and Shackleton*, 1995; *Auffret et al.*, 1996; *Rosell-Melé et al.*, 1997; *Lebreiro et al.*, 1997]. High sea surface productivity during HEs could have been created by the mixing of deep nutrient-rich waters with surface waters during the iceberg drifting [*Sancetta*, 1992]. Decreases in productivity at the beginning and at the end of the event may be explained by rapid changes of SST and SSS. Analysis of coccoliths on core MD 952042 by *Bouldoire et al.* [1996] shows a strong increase of the species *Floripheara profunda* during HEs. Since this species lives in the lower photic zone its increase in relative abundance in the sediment is interpreted as a productivity decrease in the upper photic zone. Drops in productivity during HEs such as those indicated by coccoliths in core MD 952042 are commonly attributed to the dramatic salinity decrease and/or to the limitation of light penetration caused by suspended material and sea ice cover. The absence of foraminiferal productivity decrease during HEs could be explained by the fact that subpolar species as *G. bulloides*, *T. quinqueloba*, and left-coiling *N. pachyderma*, which are adapted to cold and low-saline Arctic and polar water masses, are less sensitive than coccoliths to the hydrographic perturbations induced by HEs.

6. Conclusion

Quantitative analysis of the planktonic foraminiferal fauna from core MD 952042 provides reliable reconstructions of regional temperature and salinity changes of the surface waters throughout the past 140 kyr. Our study indicates that changes in the environment of the Portuguese Margin during the glacial cycle have been dominated by the migration of the polar front, the occurrence of abrupt iceberg discharge events, and the evolution of continental climate in Iberia. During major cooling episodes, iceberg discharge have produced the strongest imprint on the environmental record, while during the remainder of time, variations in the regional precipitation/evaporation regime on both oceanic and continental area could exercise an influence on the salinity signal.

Our paleoceanographic reconstructions allow for the identification of 11 major cold episodes which are characterized by high abundances of the subpolar species of

planktonic foraminifera, cold SSTs (near 5°C in winter and 10°C in summer), and low salinities (anomalies ranging from -0.8 to -2.1‰). The six youngest of these cold episodes are characterized by high magnetic susceptibility and the occurrence of IRDs in the sediment. They correspond with HEs and fully document the extension of the flow of iceberg down to the southern Portuguese Margin during each of these six episodes as well as the southward migration of the polar front. The five older cold and low-salinity events occurring during stage 6, transition 6/5, glacial interstadials 5d and 5b, and at the very end of stage 5 are dated 140, 129, 110, 90, and 81 ka, respectively. Most of them show high magnetic susceptibility levels and can be considered as older HEs despite the fact that they have not always been identified in cores located farther north.

The quantitative analysis of the foraminiferal fauna allows for the characterization of three cooling steps for the cold events: (1) the dominance of the subpolar assemblage by *G.*

bulloides reflects a relatively moderate cooling only due to the input of meltwater; (2) the dominance of left-coiling *N. pachyderma* represents the interval of the most intense cooling with the installation of a polar environment; and (3) high abundances of *T. quinqueloba* characterize the first step of the warming at the end of the event and may represent the passage of the Arctic front. The sea surface productivity seems high during HE1 when left-coiling *N. pachyderma* dominates.

References

Auffret, G.A., A. Boelaert, C. Vergnaud-Grazzini, C. Müller, and R. Kerbrat, Identification of Heinrich layers in cores KS 01 north-eastern Atlantic (46°N, 17°W), implications for their origin, *Mar. Geol. 131*, 5-20, 1996.

Bard, E., M. Arnold, P. Maurice, J. Duprat, J. Moyes, and J.C. Duplessy, Retreat velocity of the North Atlantic polar front during the last deglaciation determined by accelerator mass spectrometry, *Nature, 328*, 791-794, 1987.

Bard, E., R.G. Fairbanks, M. Arnold, P. Maurice, J. Duprat, J. Moyes, and J.P. Duplessy, Sea-level estimated during the last deglaciation based on d^{18}O and accelerator mass spectrometry ^{14}C ages measured in *Globigerina bulloides, Quat. Res., 31*, 381-391, 1989.

Bard, E., B. Hamelin, M. Arnold, L. Montaggioni, G. Cabioch, G. Faure, and F. Rougerie, Deglacial sea-level record from Tahiti corals and the timing of global meltwater discharge, *Nature, 382*, 241-244, 1996.

Bé, A.W.E., and D.S. Tolderlund, Distribution and ecology of living planktonic foraminifera in surface waters of the Atlantic and Indian Oceans, in *The Micropalaeontology of Oceans*, edited by B.M. Funnell and W.R. Riedel, pp. 105-149, Cambridge Univ. Press, New York, 1971.

Boelaert, A., Variabilité de la circulation de surface et intermédiaire aux moyennes latitudes de l'Atlantique Nord: Réponse aux variations lentes et rapides du climat lors du dernier cycle glaciaire-interglaciaire, Ph. D. thesis, 160pp., Univ. de Bretagne Occidentale, Brest, France, 1998.

Bond, G., and R. Lotti, Iceberg discharges into the North Atlantic on millennial time scales during the last glaciation, *Science, 267*, 1005-1010, 1995.

Bond, G., et al., Evidence for massive discharges of icebergs into the glacial

northern Atlantic, *Nature, 360*, 245-249, 1992.

Bond, G., et al., Correlations between climate records from North Atlantic sediments and Greenland ice, *Nature, 365*, 143-147, 1993.

Bond, G., et al., A pervasive millenial-scale cycle in North Atlantic Holocene and glacial climate, *Science, 278*, 1257-1266, 1997.

Bouldoire, X., L. Beaufort, O. Cayre, E. Vincent, Y. Lancelot, and N.J. Shackleton, Stratification of the photic zone in the North Atlantic during Heinrich events recorded by planktonic microfossils, *ES Trans. AGU, 77*, (46), F21, *Fall Meet. Suppl.*, 1996.

Broecker, W.S., Massive iceberg discharges as triggers for global climate change, *Nature, 372*, 421-424, 1994.

Broecker, W.S., and G.H. Denton, The role of ocean-atmosphere reorganizations in glacial cycles, *Geoch. et Cosmochim. Acta, 53*, 2465-2501, 1989.

Broecker, W.S., G. Bond, M. Klas, E. Clark, and J. McManus, Origin of the northern Atlantic's Heinrich events, *Clim. Dyn., 6*, 265-273, 1992.

Candon, L., N. Thouveny, O. Cayre, Y. Lancelot, E. Vincent, F. Rostek, D. Pailler, E. Bard, and N.J. Shackleton, Heinrich events and organic carbon signatures deciphered by sedimentary magnetism, *ES Trans. AGU, 77*, (46), F21, *Fall Meet. Suppl.*, 1996.

Cayre, O., L. Beaufort, and E. Vincent, Paleoproductivity in the equatorial Indian Ocean for the last 260,000 yr: A transfer function based on planktonic foraminifera, *Quat. Sci. Rev.*, in press, 1999.

Chapman, M.R., and N.J. Shackleton, The effect of ice-rafting on sea surface conditions in the mid latitude North Atlantic during the last 150.000 years, paper presented at the Fifth International

Conference on Paleoceanography (ICP V), Halifax, Nova Scotia, Canada, 1995.

Climate: Long-Range Investigation, Mapping, and Prediction (CLIMAP) Members, Seasonal reconstructions of the Earth's surface at the Last Glacial Maximum. *Geol. Soc. Am., Map Chart Ser., MC-36*, 1-18, 1981.

Cortijo, E., La variabilité climatique rapide dans l'Atlantique Nord depuis 128 000 ans: Relations entre les calottes de glace et l'océan de surface, Ph. D. thesis, 235 pp. Université Paris XI, Paris, France, 1995.

Cortijo, E., et al., Changes in sea surface hydrology associated with Heinrich event 4 in the North Atlantic Ocean between 40° and 60°N, *Earth Planet. Sci. Lett. 146*, 29-45, 1997.

Cremer, M., F. Grousset, J.C. Faugères, J. Duprat, and E. Gonthier, Sediment flux patterns in the northeastern Atlantic: Variability since the Last Interglacial, *Mar. Geol., 104*, 31-53, 1992.

Dansgaard, W., et al., A new Greenland deep ice core, *Science, 218*, 1273-1277, 1982.

Dansgaard, W., et al., Evidence for general instability of past climate from a 250 kyr ice-core record, *Nature, 364*, 218-220, 1993.

Duplessy, J.C., L. Labeyrie, A. Juillet-Leclerc, F. Maitre, J. Duprat, and M. Sarnthein, Surface salinity reconstruction of the North Atlantic Ocean during the last glacial maximum, *Oceanol. Acta, 14*, 311-324, 1991.

Duplessy, J.C., L.B. Labeyrie, M. Arnold, M. Paterne, J. Duprat, and T.C.E. van Weering, Changes in surface salinity of the North Atlantic Ocean during the last deglaciation, *Nature, 358*, 485-487, 1992.

Duplessy, J.C., E. Bard, L. Labeyrie, J. Duprat, and J. Moyes, Oxygen isotope records and salinity changes in the northeastern Atlantic Ocean during the last 18,000 years, *Paleoceanography, 8*, 341-350, 1993.

Elliot, M., L. Labeyrie, G. Bond, E. Cortijo, J.L. Turon, N. Tisnerat, and J.C. Duplessy, Millenial-scale iceberg discharges in the Irminger Basin during the last glacial period: Relationship with the Heinrich events and environmental settings, *Paleoceanography, 13*, 433-446, 1998.

Erez, J., and B. Luz, Experimental paleotemperature equation for planktonic foraminifera, *Geoch. et Cosmochim. Acta, 47*, 1025-1031, 1983.

Fairbanks, R.G., A 17 000 year glacio-eustatic sea level record: Influence of glacial melting rates on the Younger Dryas event and deep-ocean circulation, *Nature, 342*, 637-642, 1989.

Fatela, F., Contribution des foraminifères benthiques profonds à la reconstitution des paléoenvironnements du Quaternaire récent de la Marge Ouest Ibérique (Marge Nord Portugaise et Banc de Galice), Ph. D. thesis, 262 pp., Univ. Bordeaux I, Bordeaux, France, 1995.

Fillon, R.H., Northwest Labrador Sea stratigraphy, sand input and paleoceanography during the last 160 000 years, in *Quaternary Environments: Eastern Canadian Arctic, Baffin Bay and Western Greenland*, edited by X. Andrew, pp. 210-247, Allen and Unwin, Winchester, Mass., 1985.

Grousset, F.E., L. Labeyrie, J.A. Sinko, M. Cremer, G. Bond, J. Duprat, E. Cortijo, and S. Huon, Patterns of ice-rafted detritus in the glacial North Atlantic (40-55°N), *Paleoceanography, 8*, 175-192, 1993.

Heinrich, H., Origin and consequences of cyclic ice rafting in the northeast Atlantic Ocean during the past 130 000 years. *Quat. Res., 29*, 142-152, 1988.

Hemleben, C., M. Spindler, and O.R. Anderson (Eds.), *Modern Planktonic Foraminifera*, 363 pp., Springer-Verlag, New York, 1988.

Hutson, W.H., The Agulhas Current during the late Pleistocene: Analysis of modern faunal analogs, *Science, 207*, 64-66, 1979.

Imbrie, J., and N.G. Kipp, A new micropaleontological method for quantitative paleoclimatology: Application to a late Pleistocene Caribbean core, in *The Late Cenozoic Glacial Ages*, edited by K.K. Turekian, pp. 71-181, Yale Univ. Press, New Haven, 1971.

Johannessen, T., E. Jansen, A. Flatoy, and C. Ravelo, The relationship between surface water masses, oceanographic fronts and paleoclimatic proxies in surface sediments of the Greenland, Iceland and Norwegian Seas, in *Carbon Cycling in the Glacial Ocean: Constraints on the Ocean's Role in Global Change, NATO ASI Ser.* vol. I 17, pp. 61-85, Springer-Verlag, New York, 1994.

Johnsen, S.J., H.B. Clausen, W. Dansgaard, K. Fuhrer, N. Gundestrup, C.U. Hammer, P. Iversen, J. Jouzel, B. Stauffer, and J.P. Steffensen, Irregular glacial interstadials recorded in a new Greenland ice core, *Nature, 359*, 311-313, 1992.

Kiefer, T., Produktivität und Temperaturen im subtropischen Nordatlantik: Zyklische und abrupte Veränderungen im späten

Quartär, Ph. D. thesis, Kiel Univ., Kiel, Germany, 1997.

Kiefer, T., F. Abrantes, M. Sarthein, M. Weinelt, and L. Labeyrie, Prominent productivity spikes in the subtropical North Atlantic parallel Heinrich meltwater events, paper presented at the Fifth International Conference on Paleoceanography (ICP V), 85, Halifax, Nova Scotia, Canada, 1995.

Kipp, N.G., New transfer function for estimating past sea-surface condition from sea-bed distribution of planktonic foraminiferal assemblages in North Atlantic, in *Investigation of Late Quaternary Paleoceanography and Paleoclimatology*, edited by R.M. Cline and J.D. Hays, *Geol. Soc. Am. Mem. 145*, 3-41, 1976.

Kudrass, H.R., and J. Thiede, Statigraphische Untersuchungen an Sedimentkernen des ibero-marokkanischen Kontinentalrandes, *Geol. Rundsch., 60*, 294-391, 1970.

Labeyrie, L.D., J.C. Duplessy, and P.L. Blanc, Variations in mode of formation and temperature of oceanic deep waters over the past 125 000 years, *Nature, 327*, 477-482, 1987.

Lebreiro, S.M., J.C. Moreno, I.N. McCave, and P.P.E. Weaver, Evidence for Heinrich layers off Portugal (Tore Seamount: 39°N, 12°W), *Mar. Geol., 131*, 47-56, 1996.

Lebreiro, S.M., J.C. Moreno, F. Abrantes, and U. Pflaumann, Productivity and paleoceanographic implications on the Tore Seamount (Iberian Margin) during the last 225 kyr: Foraminiferal evidence, *Paleoceanography, 12*, 718-727, 1997.

Levitus, S., Climatological atlas of the World Ocean. *NOAA Prof. Pap. 13*, 173 pp. U.S. Gov. Print. off., Washington, D.C., 1982.

Little, M.G., R. Schneider, D. Kroon, B. Price, C.P. Summerhayes, and M. Segl, Trade wind forcing to sub-Milankovitch climate variability, *Paleoceanography, 12*, 568-576, 1997.

Manighetti, B., I.N. McCave, M. Maslin, and N.J. Shackleton, Chronology for climate change: Developing age models for the biogeochemical ocean flux study cores, *Paleoceanography, 10*, 513-525, 1995.

Martinson, D.G., N.G. Pisias, J.D. Hays, J. Imbrie, C. T. Moore, Jr., and N.J. Shackleton, Age dating and the orbital theory of the ice ages : Development of a high-resolution 0 to 300,000-year chronostratigraphy, *Quat. Res., 27*, 1-29, 1987.

Maslin, M.A., N.J. Shackleton, and U. Pflaumann, Surface water temperature, salinity and density changes in the northeast Atlantic during the last 45 000 years: Heinrich events, deep water formation, and climatic rebounds, *Paleoceanography, 10*, 527-544, 1995.

Mix, A.C., and W.F. Ruddiman, Structure and timing of the last deglaciation: Oxygen-isotope evidence, *Quat. Sci. Rev., 4*, 59-108, 1985.

Ottens, J.J., Planktonic foraminifera as indicators of ocean environments in the northeast Atlantic, Ph. D. thesis, 189 pp.,

Urije Univ., Amsterdam, Netherlands, 1992.

Pastouret, L., G.A. Auffret, M. Hoffert, M. Melguen, H.D. Needham, and C. Latouche, Sédimentation sur la ride de Terre-Neuve, *Can. J. Earth Sci., 12*, 1019-1035, 1975.

Pflaumann, U., J. Duprat, C. Pujol, and L.D. Labeyrie, SIMMAX: A modern analog technic to deduce Atlantic sea surface temperatures from planktonic foraminifera in deep-sea sediments, *Paleoceanography, 11*, 15-35, 1996.

Pickard, G.L., and W.J. Emery, *Descriptive Physical Oceanography: An introduction*, 4th ed., 249 pp., Pergamon Press, Tarrytown, N.Y., 1982.

Pons, A., and M. Reille, The Holocene and upper Pleistocene pollen record from Padul (Granada, Spain): A new study, *Palaeogeogr., Palaeoclimatol., Palaeoecol., 66*, 243-263, 1988.

Prell, W.L., The stability of low-latitude sea-surface temperatures: An evaluation of the CLIMAP reconstruction with emphasis on the positive SST anomalies, *technical report*, 60 pp., Dep. of Appl. Sci., Brown University, Providence, R.I., 1985.

Pujol, C., Les foraminifères planctoniques de l'Atlantique Nord au Quaternaire. Ecologie, Stratigraphie, Environnement, Ph. D. thesis, 254 pp., Univ. Bordeaux I, Bordeaux, France, 1980.

Rasmunssen, T.L., E. Thomsen, T.C.E. van Weering, and L. Labeyrie, Rapid changes in surface and deep water conditions at the Faeroe Margin during the last 58,000 years, *Paleoceanography, 11*, 757-771, 1996.

Rasmunssen, T.L., T.C.E. van Weering, and L. Labeyrie, Climatic instability, ice sheets and ocean dynamics at high northern latitudes during the last glacial period (58-10 KA BP), *Quat. Sci. Rev., 16*, 71-80, 1997.

Revel, M., J.A. Sinko, F.E. Grousset, and P.E. Biscaye, Sr and Nd isotopes as tracers of North Atlantic lithic particles: Paleoclimatic implications, *Paleoceanography, 11*, 95-113, 1996.

Robinson, S.G., M.A. Maslin, and I.N. McCave, Magnetic susceptibility variations in upper Pleistocene deep-sea sediments of the NE Atlantic: Implications for ice rafting and paleocirculation at the Last Glacial Maximum, *Paleoceanography, 10*, 221-250, 1995.

Rosell-Melé, A., M.A. Maslin, J.R. Maxwell, and P. Schaeffer, Biomarker evidence for "Heinrich" events, *Geoch. et Cosmochim. Acta, 61*, 1671-1678, 1997.

Rostek, F., G. Ruhland, F.C. Bassinot, P.J. Müller, L.D. Labeyrie, Y. Lancelot, and E. Bard, Reconstructing sea surface temperature and salinity using $d^{18}O$ and alkenone records, *Nature, 364*, 319-321, 1993.

Ruddiman, W.F., Northern oceans, in *The Geology of North America*, vol. K3, *North America and Adjacent Oceans During the Last Deglaciation*, edited by W.F. Ruddiman, Geol. Soc. of Am., pp 137-154, Boulder, Colo., 1987.

Ruddiman, W.F., and A. McIntyre, The North Atlantic Ocean during the last deglaciation, *Palaeogeogr., Palaeoclimatol., Palaeoecol., 35*, 145-214, 1981.

Sancetta, C., Primary production in the glacial North Atlantic and North Pacific Oceans, *Nature, 360*, 249-251, 1992.

Thioulouse, J., MacMul and GraphMu: two Macintosh programs for the display and analysis of multivariate data, *Comp. Geosci., 16*, 1235-1240, 1990.

Thomas, E., L. Booth, M. Maslin, and N.J. Shackleton, Northeastern Atlantic benthic foraminifera during the last 45,000 years: Changes in productivity seen from the bottom up, *Paleoceanography, 10*, 545-562, 1995.

van Kreveld, S.A., Northeast Atlantic late Quaternary planktic foraminifera as primary productivity and water mass indicators, *Scr. Geol., 113*, 24-91, 1996.

van Kreveld, S.A., M. Knappertsbusch, J.J. Ottens, G. Ganssen, and J.E. van Hinte, Biogenic carbonate and ice rafted debris (Heinrich layers) accumulation in deep sea sediments from a northeast Atlantic piston core, *Mar. Geol., 131*, 21-46, 1996.

Voelker, A.H.L., M. Sarnthein, P.M. Grootes, H. Erlenkeuser, C. Laj, A. Mazaud, M.J. Nadeau and M. Schleicher, Correlation of marine ^{14}C ages from the Nordic Seas with the GISP2 isotope record: Implications for radiocarbon calibration beyond 25 ka BP, *Radiocarbon, 40*, 517-534, 1998.

Zahn, R., J. Schönfeld, H.-R. Kudrass, M.-H. Park, H. Erlenkeuser, and P. Grootes, Thermohaline instability in the North Atlantic during meltwater events: Stable isotope and ice-rafted detritus records from SO75-26KL, Portuguese margin, *Paleoceanography, 12*, 696-710, 1997.

O. Cayre, Laboratoire de Géologie du Quaternaire du CNRS, CEREGE, BP 80, 13545 Aix en Provence Cedex 4, France. (ocayre@cerege.fr)

M.A. Hall, Godwin Laboratory, University of Cambridge, Cambridge CB2 3RS, England, U.K.

Y. Lancelot and E. Vincent, Centre d'oceanologie de Marseille, Case 901-Campus de Luminy, 13288 Marseille Cedex 9, France.